KEK-PREPRINT-92-36

Fermilab Library
0 1160 0009185 4

KEK Preprint 92-36
AMY 92-1
May 1992
H

e^+e^- ANNIHILATION INTO FOUR-LEPTON FINAL STATES WITH THE AMY DETECTOR

TADAO NOZAKI

Department of Physics
Nat. Lab. for High Energy Physics (KEK)
Tsukuba, Ibaraki, 305, Japan

ABSTRACT

We report the latest results of a study of single and double-tag events with four-lepton final states produced in e^+e^- collisions at center-of-mass energies from 50 to 61.4 GeV using the AMY detector at TRISTAN.

ROUTE TO
NAME
LOCATION
RETURN TO

Talk given at the IXth International Workshop on Photon-Photon Collisions, March 22-26, 1992, University of California, San Diego.

National Laboratory for High Energy Physics, 1992

KEK Reports are available from:

Technical Information & Library
National Laboratory for High Energy Physics
1-1 Oho, Tsukuba-shi
Ibaraki-ken, 305
JAPAN

Phone: 0298-64-1171
Telex: 3652-534 (Domestic)
(0)3652-534 (International)
Fax: 0298-64-4604
Cable: KEKOHO

e^+e^- ANNIHILATION INTO FOUR-LEPTON FINAL STATES WITH THE AMY DETECTOR

TADAO NOZAKI

(representing the AMY Collaboration)

Department of Physics
Nat. Lab. for High Energy Physics (KEK)
Tsukuba, Ibaraki, 305, Japan

ABSTRACT

We report the latest results of a study of single and double-tag events with four-lepton final states produced in e^+e^- collisions at center-of-mass energies from 50 to 61.4 GeV using the AMY detector at TRISTAN.

1. Introduction

In this report we present measured cross sections for the $e^+e^- \to e^+e^-e^+e^-$ and $e^+e^- \to e^+e^-\mu^+\mu^-$ processes and compare them with the prediction of Quantum Electrodynamics (QED). The data samples were obtained with the AMY detector at the TRISTAN at center-of-mass energies from 50 to 61.4 GeV. The lowest order Feynman diagrams that contribute to these processes can be classified into four groups: multiperipheral, bremsstrahlung, conversion, and annihilationas as shown in Fig. 1.

The QED expectation is that these diagrams and their radiative corrections should account for the observed cross sections to high precision. Previous studies of the processes $e^+e^- \to e^+e^-\ell^+\ell^-$ (ℓ = e, or μ) at the lower energies of the PEP and PETRA colliders have shown no discrepancies with QED.[1] However, our previous study of the same processes for the integrated luminosity of 33.8 pb^{-1} has shown some discrepancies with QED as described below.[2] For the cases where two or three tracks are produced at wide angles the cross sections agreed well with theory, but we observed a significant excess of $e^+e^- \to e^+e^-\mu^+\mu^-$ events with four tracks at wide angles.[2] After the publication of ref.2 we upgraded the AMY detector from AMY1.0 to AMY1.5. One of the major changes is the replacement of the endcap calorimeters consisting of the two different sets of calorimeters of PTC and RSC by a single set of calorimeter of ESC. Since then we have accumulated about twice more integrated luminosity. For $e^+e^- \to e^+e^-\mu^+\mu^-$ process all the available data of 95.7 pb^{-1} were analyzed, but for $e^+e^- \to e^+e^-e^+e^-$ process only 61.0 pb^{-1}m data were analyzed. In this report we update the previous results using these data.

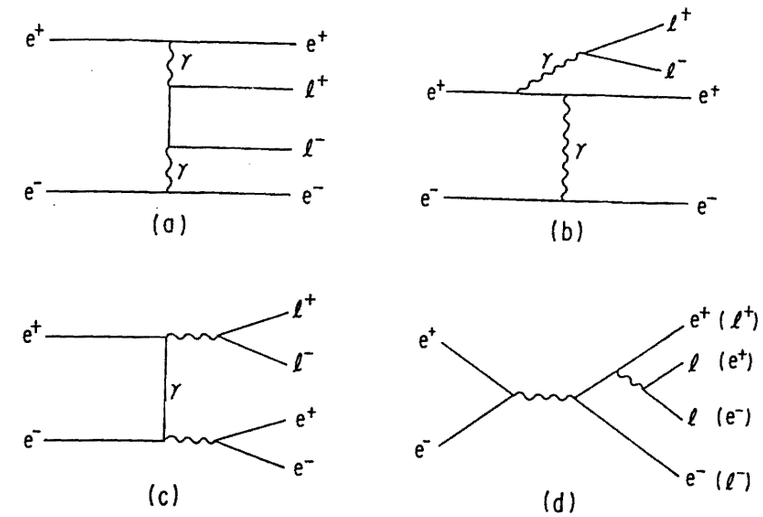

Fig. 1. The four classes of lowest-order Feynman graphs for the reactions $e^+e^- \to e^+e^-\ell^+\ell^-$: (a)multiperipheral, (b)bremsstrahlung, (c)conversion, and (d)annihilation.

2. Classification of Events

For discussion and analysis we partition the $e^+e^- \to e^+e^-\ell^+\ell^-$ events according to observed topology into untagged, single-tag, and double-tag subsamples. For untagged kinematics, both of the final e^+ and e^- are unobserved in the detector because they emerge at a small angle relative to the beam axis where detector coverage is incomplete. If one or both of the final electrons emerge at an angle large enough for detection, the event is respectively a single-tag or double-tag event. In this report we only present results for single-tag or double-tag events. The ℓ^+ and ℓ^- are measured in all cases. This subdivision by topology is convenient for data analysis and, more importantly, reflects the radically different relative contributions of the groups of Feynman graphs to the different kinematic regimes. Table 1 shows these relative contributions, excluding interference, for the kinematic cuts adopted for our analysis.

3. Event Selection

We show a schematic view of the latest AMY detector (AMY1.5) in Fig 2. A detailed description of the AMY detector is given in ref.3. In brief, the momenta of secondary charged particles in the solid angle $|\cos\theta| < 0.883$ are measured in an open cell cylindrical drift chamber (CDC). A cylindrical electromagnetic calorimeter (SHC), also within the the magnetic field volume, covers the angular range $|\cos\theta| < 0.731$. Endcap calorimeters cover the angular range $0.777 < |\cos\theta| < 0.982$ (ESC) for the latest detector configuration (AMY1.5) and angular ranges $0.777 < |\cos\theta| < 0.899$ (RSC) and $0.899 < |\cos\theta| < 0.966$ (PTC) for the previous detector configuration

Table 1. Relative contribution to the cross section for the 4-lepton processes under various experimental tagging condition (by requiring number of visible tracks above 28°). The interference between the different Feynman groups is not included.

	Multi-peripheral	Brems-strahlung	Con-version	Anni-hilation
untagged (2 tracks)	~ 100%	~ 0%	~ 0%	~ 0%
single-tag (3 tracks)	~ 83%	~ 17%	~ 0%	~ 0%
double-tag (4 tracks)	~ 10%	~ 80%	~ 6%	~ 4%

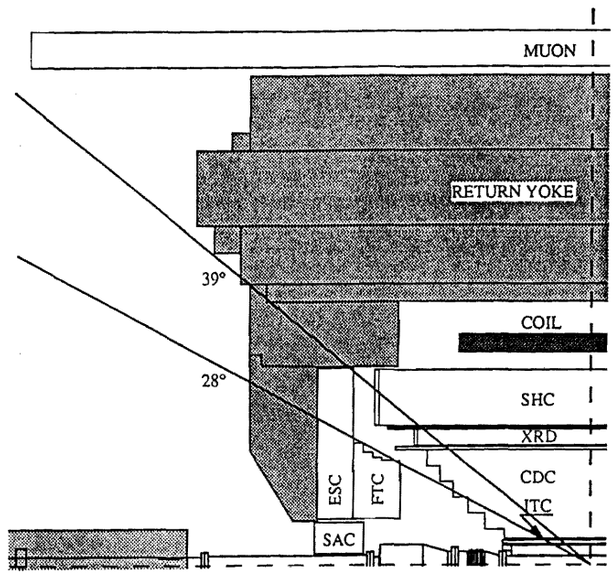

Fig. 2. A schematic view of the latest AMY detector (AMY1.5)

(AMY1.0). The corresponding fractions of the data sample for AMY1.0 and AMY1.5 are about 30% and 50% for $e^+e^- \to e^+e^-\mu^+\mu^-$ and $e^+e^- \to e^+e^-e^+e^-$, respectively The angular region is divided into the central region of $|\cos\theta| < 0.731$ and the endcap region of $0.777 < |\cos\theta| < 0.883$. The endcap region is chosen to be smaller than

the acceptance of the endcap detectors due to the limited angular acceptance of the CDC. The number of Bhabha events ($e^+e^- \to e^+e^-$) observed in the ESC or PTC, appropriately scaled, is our measure of integrated luminosity. The SHC and ESC (or RSC and PTC) are the principal tools for electron identification. The electron criteria are: $E/p > 0.5$ and $p > 2.0$ GeV/c where E may be measured in the endcap calorimeters or the SHC. These criteria are 98% efficient. The probability that a charged pion is misidentified as an electron is about 1.3% at 1.0 GeV/c and drops to 0.2% at 5 GeV/c.

We identify tracks measured in the CDC as muons when they penetrate the SHC and the iron flux return yoke, a total of about 9 nuclear interaction lengths at 90°. Four layers of planar drift chambers at the outer surface of the yoke measure the exit location of penetrating tracks, and an adjacent layer of scintillation counters measures the transit time relative to beam-crossing time. These detector elements cover the solid angle $|\cos\theta| < 0.731$. To suppress contamination from cosmic rays we require the scintillator time to be consistent with a track produced at the beam crossing. For muons with momentum above 3.0 GeV/c and within the fiducial cuts of the muon detection system, the muon identification efficiency is about 83%. In hadronic events misidentification of charged pions and kaons as muons occurs at the respective rates of $\simeq 1.3\%/p(\mathrm{GeV/c})$ and $\simeq 6\%/p$ primarily as a result of decay-in-flight. Muons are required to have $p > 2.0$ GeV/c. In the case that an event has one muon identified by penetration through the yoke (positive identification), minimum energy deposition in a calorimeter, i.e. $E/p < 0.5$, is sufficient to confirm that a second track is also a muon.

Potentially serious backgrounds arise from the processes $e^+e^- \to e^+e^-\gamma$ and $e^+e^- \to \mu^+\mu^-\gamma$ followed by pair conversion of the γ in the beam pipe. We suppress these events by the requirement that the invariant mass of any e^+e^- pair exceed 1.0 GeV/c^2. We forgo an analogous cut on the invariant mass of muon pairs. It would be superfluous because less than 10^{-4} of γ conversions in the beam pipe produce a $\mu^+\mu^-$ pair, and the contamination expected from this process is in any case less than 0.001 events in any of our three topological samples.

To qualify for the single and double-tag samples, events must have at least one electron with $p > 5$ GeV/c in the central or endcap region and two muons (at least one is positively identified) with $p > 2$ GeV/c or two additional electrons with $p > 2$ GeV/c in the central region. In addition the single-tag events pass a 1-C kinematic fit[4] with $\chi^2/DOF < 40$, and their missing momentum must be within 28° of the beam axis. When the missing momentum is between 15° and 28° (3° and 28°) of the beam axis for AMY1.0 (AMY1.5) there must exist some energy deposit in the endcap detector. The double-tag events pass a 4-C kinematic fit with $\chi^2/DOF < 40$.[4] Finally we scanned graphic reconstruction of the surviving events. The numbers of events observed were 10 and 4 for the $e^+e^-e^+e^-$ single and double-tag samples and

18 and 6 for the respective $e^+e^-\mu^+\mu^-$ samples. These events have a rather distinct topology and are highly constrained;the expected contamination in these samples is less than 2 events.

4. Monte Carlo Calculations

To obtain the predictions of QED for these four-lepton processes we ran several independent Monte Carlo event generators. Two of these, both by Berends, Daverveldt, and Kleiss (BDK), use the same general methods but are tailored for the single-tag and double-tag kinematics.[5] The BDK codes incorporate all four groups of Feynman graphs and allow fully for their interference. The code for double-tag kinematics also incorporates Z exchange in some of the graphs. The generator by Vermaseren incorporates only the multiperipheral and bremsstrahlung graphs.[6] which is adequate for untagged and single-tag cross sections. One generator by Kuroda handles the untagged kinematics using only the multiperipheral and bremsstrahlung graphs.[7] A second generator by Kuroda, which incorporates only the conversion and annihilation diagrams, supplements the Vermaseren calculation for the double-tag kinematics.[8] The cross sections we obtain for the groups of Feynman graphs taken separately are consistent among the various generators. The Kuroda's generator is easier to calculate efficiency than the BDK generator since the former creates events with the same weights while the latter with different weights. Therefore at first we calculated efficiency and acceptance of events for each mass bin of lepton pairs using results of detector simulation for events created by Kuroda's first generator. Secondly the diffential cross section after the event selection cuts was calculated at the four-vector level using the BDK generator. Finally two results were combined to obtain the diffential cross section corrected for detector acceptance and efficiency.

The numbers of events which the QED codes predict for our integrated luminosity are 5.7 and 2.5 for the $e^+e^-e^+e^-$ single and double-tag samples and 14.4 and 2.8 for the respective $e^+e^-\mu^+\mu^-$ samples. These data are listed together with our data in Table 2. Also listed in the Table 2 are the results corresponding to the early (AMY1.0) and later parts (AMY1.5) of the data sample. It is to be noted that the early data were reanalyzed with the new cuts. The observed number of events are consistent with the QED predictions within the errors although the data are slightly larger than the predictions.

5. Results

In Figs. 3a and 3b we show the distributions of e^+e^- and $\mu^+\mu^-$ invariant mass, respectively. The curves in these figures are the distributions produced from the QED event generator.

For the $e^+e^-e^+e^-$ final state only the smallest e^+e^- invariant mass in each event

Table 2. (a) Summary of $e^+e^- \to e^+e^-e^+e^-$ events. N_{obs} and N_{QED} represent observed and QED predicted numbers of events, respectively.

Data sample	Before 1989 Aug	1989 Aug.-1990 Fall	Before 1990 Fall
$\int$ Ldt	33.8 pb^{-1}	27.2 pb^{-1}	61.0 pb^{-1}
$\sqrt{s}$	50-60.8 GeV	mostly 58 GeV	58, 50-60.8 GeV
Detector	AMY1.0	AMY1.5	AMY1.0 and AMY1.5
Single- and double-tag events			
N_{obs}	8	6	14
N_{QED}	4.6	3.6	8.2
N_{obs}/N_{QED}	1.8±0.6	1.7± 0.7	1.7± 0.5
Double-tag events			
N_{obs}	2	2	4
N_{QED}	1.4	1.1	2.5
N_{obs}/N_{QED}	1.5±1.0	1.8± 1.3	1.6± 0.8

is included. The data are in good agreement with QED predictions except for the first bin ($M_{\mu\mu} < 5.0$ GeV/c^2) of $e^+e^-\mu^+\mu^-$ sample, where we observe 13 events against the expected number of events of 5.6, namely the data point is two sigma higher than the prediction. For the early data sample of 33.8 pb^{-1} we observed a significant excess of $e^+e^- \to e^+e^-\mu^+\mu^-$ events with four tracks at wide angles; we observe 7 events against 1.9 expected events for the previous cuts[2] and for the present cuts we observe 6 events against 1 expected event. However, for the recent data we have not observed any additional double-tag events. As a result for the total sample of data the number of observed events is still 6 while the expected number of events is 2.8. Therefore excess of events in the double-tag topology is not significant.

The present event selection criteria are more tighter than those for the previous analysis[2]. As a result the ratios of the predicted number of single-tag events for the present cuts and the previous cuts are about 1/4.6 and 1/3.2 for $e^+e^-e^+e^-$ and $e^+e^-\mu^+\mu^-$ processes, respectively. The corresponding ratios for double-tag events are 1/1.1 and 1/2, respectively. The corresponding ratios of the observed number of double tag events are 6/7 and 1/1, respectively. Namely no significant effects due to the change of the selection criteria are observed for double-tag events. Therefore no further observation of double-tag $e^+e^-\mu^+\mu^-$ events is not due to the change of the selection criteria.

Table 2. (b) Summary of $e^+e^- \to e^+e^-\mu^+\mu^-$ events. N_{obs} and N_{QED} represent observed and QED predicted numbers of events, respectively.

Data sample	Before 1989 Aug	1989 Aug.-1991 Dec	Before 1991 Dec
$\int$ Ldt	33.8 pb^{-1}	61.9 pb^{-1}	95.7 pb^{-1}
$\sqrt{s}$	50-60.8 GeV	mostly 58 GeV	58, 50-60.8 GeV
Detector	AMY1.0	AMY1.5	AMY1.0 and AMY1.5
Single- and double-tag events			
N_{obs}	14	10	24
N_{QED}	6.0	11.2	17.2
N_{obs}/N_{QED}	2.6±0.7	0.9± 0.3	1.4± 0.3
Double-tag events			
N_{obs}	6	0	6
N_{QED}	1.0	1.8	2.8
N_{obs}/N_{QED}	6.0±2.4	0.0± 1.0	2.1± 0.9

In Figs. 4a and 4b we show the polar angle distributions of muons and electrons in $e^+e^- \to e^+e^-\mu^+\mu^-$ and $e^+e^- \to e^+e^-e^+e^-$, respectively. As seen in the figures the data are consistent with the predictions.

We have studied properties of the reactions $e^+e^- \to e^+e^-e^+e^-$ and $e^+e^- \to e^+e^-\mu^+\mu^-$ where one or both of the final electrons emerge at an angle large enough for detection. We have used 95.7 and 61.0pb^{-1} samples of e^+e^- collisions, spanning center-of-mass energies from 50 to 61.4 GeV to study reactions $e^+e^- \to e^+e^-e^+e^-$ and $e^+e^- \to e^+e^-\mu^+\mu^-$, respectively. An order α^4 QED calculation is in good agreement with the results except for the case where $\mu^+\mu^-$ invariant mass is less than 5 GeV/c^2. In this case we see an excess of $e^+e^- \to e^+e^-\mu^+\mu^-$ events, but which is only a two sigma deviation and not significant.

Acknowledgements

I would like to thank D. Caldwell and H. Paar for organizing this pleasant and stimulating meeting. I specially thank T. Omori and Y. Kurihara for explaining to me details of their analysis.

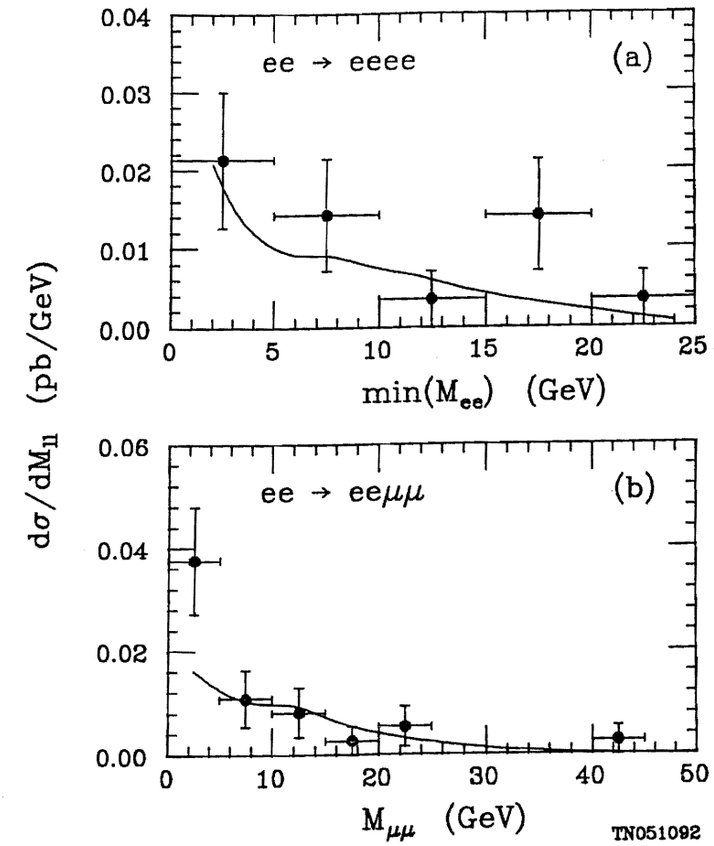

Fig. 3. (a) The invariant mass distribution of e^+e^- for $e^+e^- \to e^+e^-e^+e^-$. (b) The invariant mass distribution of $\mu^+\mu^-$ for $e^+e^- \to e^+e^-\mu^+\mu^-$. The curves in these figures are the distributions produced from the QED event generator.

REFERENCES

1. A.Petradza, Ph. D thesis, Univ. of Michigan, (1989), unpublished; H.-J. Behrend *et al.*(CELLO Collab.), Z. Phys. **C43** (12989) 1; W. Bertel *et al.*(JADE Collab.), Z. Phys.**C30** (1989) 545; B. Adeva *et al.*(Mark-J Collab.), Phys. Rev. **D38** (1988) 2665; Ch. Berger *et al.*(PLUTO Collab.), Z. Phys. **C27** (1985) 249.
2. Y.H. Ho *et al.*(AMY Collab.), Phys. Lett,**B244** (1990) 573.
3. T. Kumita *et al.*(AMY Collab.), Phys. Rev. **D42** (1990) 1339. See also: H. Sagawa *et al.*(AMY Collab.), Phys. Rev. Lett. **60** (1988) 93 and S. Igarashi *et al.*(AMY Collab.), Phys. Rev. Lett. **60** (1988) 2359.
4. O.I. Dahl *et al.*, SQUAW, LBL Group-A note P-126 (1968), unpublished.
5. F.A. Behrends, P.H. Daverveldt and R. Kleiss, Phys. Lett. **B148** (1984) 489. The code for single-tag $e^+e^-\mu^+\mu^-$ events was discussed in Comp. Phys. Comm. **40** (1986) 309.
6. J.A.M. Vermaseren, in Proc. Int. Workshop on Photon-Photon Collisions (Amiens, 1980); J.A.M. Vermaseren, Nucl. Phys. **B229** (1983) 347.
7. M. Kuroda, Meiji Gakuin Univ. (Tokyo) Research Journal **424** (1988) 27.
8. M. Kuroda, Meiji Gakuin Univ. preprint MGU-DP 7 (1988), unpublished.

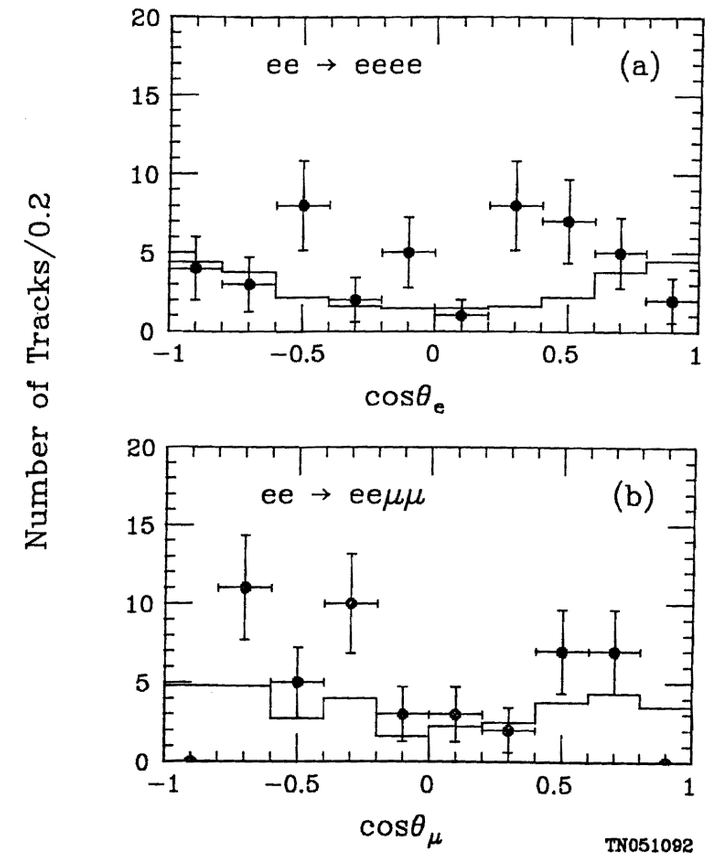

Fig. 4. (a) The polar angle distribution of $e^{\pm}$ for $e^+e^- \to e^+e^-e^+e^-$. (b) The polar angle distribution of $\mu^{\pm}$ for $e^+e^- \to e^+e^-\mu^+\mu^-$. The histograms in these figures are the distributions produced from the QED event generator.